

# Molecular dynamics simulation of synchronization in driven particles

Tiare Guerrero\* and Danielle McDermott†

*Department of Physics, Pacific University, Forest Grove, OR 97116*

(Dated: February 26, 2021)

Synchronization plays a key role in many physical processes. A particle may execute motion coordinated with position, a synchronization behavior that can be used to isolate complex natural behaviors, either with simulations or table-top experiments. We discuss a molecular dynamics simulation of a single particle moving through a viscous liquid driven across a washboard potential energy landscape. Our results show many dynamical patterns as we alter the landscape and driving force. Under certain conditions, the particle velocity and location are synchronized or phase-locked, forming closed orbits in phase space. Quasi-periodic motion is common, where the dynamical center of motion shifts the phase space orbit. We include molecular dynamics code to simulate and characterize particle dynamics.

## I. INTRODUCTION

Synchronization is a universal phenomena in which individual oscillators change frequency due to external stimuli [1]. The flickering patterns of candle flames mediated by temperature fluctuations [3], vibrations of singing wineglasses interacting through sound waves [4], and metronomes vibrating through a supporting platform [5] are examples of in-phase coupled oscillations. Biological systems benefit from cooperative synchronization – birds coordinate wing flaps to optimize energy use during flight [6], frogs alternate croaking patterns [7], humans clap in time with music [8] and at a cellular level, neurons simultaneously fire in cardiac muscle [9] and brain tissue [10]. External forcing can cause or regulate synchronization – an electrical pacemaker regulates a heart beat and a pulsed light modifies the flashing pattern of fireflies .

Synchronized phase-locking or mode-locking first appeared in the scientific literature with Huygens’ 1665 experiments on motions of synchronized pendula in wall-mounted clocks [2]. A locked-mode is an integer frequency ratio. In Huygens clocks, the pendula were observed swing at same rate – a 1:1 mode. For a higher modes, consider simple pendula of different lengths, a 2:1 mode occurs when a pendulum four times the length of another swings with twice the period.

Complex dynamics such as synchronized mode-locking can be studied with colloid particles in experiments or simulations. Typical colloids are plastic spheres suspended in de-ionized water or silica beads suspended in organic solvent. Because colloids are large and move slowly, particle position can be measured in real time with an optical camera [15]. Experimental measurements of step-by-step dynamics of colloids performing phase-locked motions are useful for understanding synchronization at a single particle level [27].

Light is a tool for manipulating the colloidal environment to alter synchronization patterns. Colloids can be

trapped with radiation pressure from a laser beam [32]. A colloid centered in an optical trap is uniformly bombarded by photons. Off-center colloids experience a net force due to uneven photon collisions across the particle surface. Depending on the location of the particle in the trap, the radiation pressure either moves colloids toward center or ejects it from the trap. Diffraction gratings can create more complex light environments, such as periodic patterns of minima suitable for synchronization studies [31].

A single particle oscillator in a potential well is like a skateboarder in a half-pipe or a child on a swing. A confined oscillator may synchronize its location to the periodic pattern of the external drive, moving back and forth in time with the beat, or moving between substrate minima. A constant or dc drive the landscape modulates the particle velocity. Below some threshold the dc force is not strong enough to push the particle across a potential maximum so the average velocity is zero, a phenomena referred to as pinning [25]. Above the pinning threshold, a particle subject to a constant drive force will increase its speed at a rate propotional to the external drive. When the applied force varies periodically, the ac drive can cause the particle to hop back and forth across the landscape minima. Many synchronized patterns occur controlled by the substrate period, leading to mode-locking, where the average particle velocity is fixed for a range of dc drive forces [26]. The model presented in this paper resembles an overdamped driven pendulum.

Here we perform numerical studies on the synchronized dynamics of confined particles driven over a washboard shaped potential energy landscape. We describe our molecular dynamics model for a single particle in Section II, The model closely resembles a damped driven pendulum, and is easy to simulate yet relevant to condensed matter systems. We summarize our results including synchronized motion of a single confined particle driven across a periodic landscape in Section III. We include exercises for interested students in Section IV. In Section V we describe how our results apply to physical systems such as dusty plasmas, superconducting vortices and Josephson junctions.

---

\*Electronic address: [guer9330@pacificu.edu](mailto:guer9330@pacificu.edu)

†Electronic address: [mcdermott@pacificu.edu](mailto:mcdermott@pacificu.edu)

## II. MOLECULAR DYNAMICS SIMULATION

We use a classical model for studying the dynamics of  $N$  interacting particles, using the net force on each particle to calculate its trajectory. Particles are confined in a two-dimensional (2D) simulation of area  $A = L \times L$  where  $L = 46.6a_0$  where  $a_0$  is a dimensionless unit of length. An individual particle  $i$  has position  $\vec{r}_i = x_i\hat{x} + y_i\hat{y}$  and velocity  $\vec{v}_i = d\vec{r}_i/dt$ . The edges of the system are treated with periodic boundary conditions such that a particle leaving the edge of the system is mapped back to a position within the simulation boundaries by the transformation  $x_i + L \rightarrow x_i$  and  $y_i + L \rightarrow y_i$ . We show a schematic of the system in Fig. 1(a). The units of the simulated variables are summarized in Table I.

We confine the particles using a position dependent potential energy function, called a landscape or substrate. The landscape is modulated in the  $y$ -direction with the periodic function

$$U(y) = U_0 \cos(2\pi y/\lambda) \quad (1)$$

where  $\lambda = L/N_p$  with  $N_p$  are the number of periods, and  $U_0$  is an adjustable parameter to set the depth of the minima with simulation units of energy  $E_0$ . We plot this function in Fig. 1 for  $N_p = 3$ . In Fig. 1(a) we show the  $x - y$  plane with a contour plot of  $U(y)$  to illustrate the 2D potential energy landscape, where the maxima are colored red and the minima colored blue. The confining force on a particle  $i$  is calculated as  $\vec{F}_i^l(\vec{r}_i) = -\nabla U_l(\vec{r}_i)$ . In Fig. 1(b) we plot the function  $U(y)$  to illustrate how the magnitude  $\vec{F}_i^l$  is calculated from particle position  $y_i$ .

Particles are subject an external time-dependent driving force  $\vec{F}^d(t)$  applied parallel to the  $y$ -direction. We model this force as

$$\vec{F}^d(t) = [F^{dc} + F^{ac} \sin(\omega t)]\hat{y}, \quad (2)$$

with a constant component  $F^{dc}$ , a time dependent component with amplitude  $F^{ac}$  and frequency  $\omega = 2\pi f$ . The inertia of small particles is reduced by interactions with fluid particles [16]. We assume colloids are overdamped – suspended in a continuous viscous fluid that dissipates energy so the particles do not accelerate. Newton's second law for an individual particle is simplified by the assumption  $\vec{a}_i$  is zero. The overdamped equation of motion for the velocity  $\vec{v}_i$  of an isolated particle is

$$\eta \vec{v}_i = \vec{F}_i^l(\vec{r}_i) + \vec{F}^d(t). \quad (3)$$

with friction coefficient  $\eta = 1$  in units of  $v_0/F_0$ . The term  $-\eta \vec{v}_i$  is a drag force used model energy dissipation from the fluid. We discuss friction models for spheres moving through fluids in Exercise IV A.

The equation of motion provides a direct calculation of the velocity of an individual particle from location  $\vec{r}_i$  and the simulation time. The molecular dynamics simulation is controlled by a *for*() loop which runs from an initial to maximum integer number of time steps. At each time

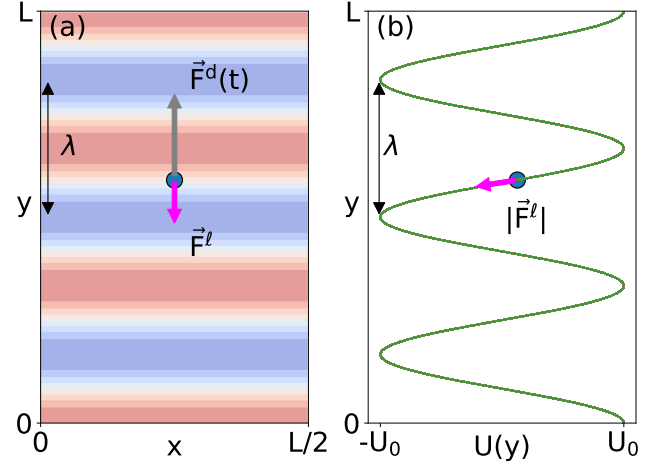


FIG. 1: Schematic of the simulation of a single particle driven across a washboard potential energy landscape. (a) View of the  $x - y$  plane. The time-dependent applied driving force  $\vec{F}^d$  is parallel to the  $y$ -axis. The landscape is shown with maxima in the potential energy marked in red and minima marked in blue. A particle is subject to competing forces of the landscape and applied driving force. (b) The potential energy function along the  $y$ -axis  $U_l(y)$ . The particle in (a) is shown at the same  $y$ -position. The slope of  $U_l(y)$  is the magnitude of force  $\vec{F}^l$ .

step we evaluate the net force on each particle as a function of its position  $\vec{r}_i(t)$  and then integrate the equation of motion to move particles to an updated position. Since the acceleration is zero, the integration of the equation of motion is performed via the Euler method

$$\vec{r}_i(t + \Delta t) = \vec{v}_i(t)\Delta t + \vec{r}_i(t) \quad (4)$$

for a time step  $\Delta t = 0.1\tau$ . In Exercise IV C we describe the numerical methods for solving differential equations.

## III. MODE-LOCKING OF A SINGLE PARTICLE

Here we drive a single particle across the landscape. The numerical implementation of the landscape is calculated with Eq. 1 as

$$F_y^l(y) = -A_p \sin(2\pi y/\lambda) \quad (5)$$

where the force is scaled with parameter  $A_p = 2\pi U_0/\lambda$ . In this section we fix the landscape parameters to  $A_p = 0.1F_0$  with  $N_p = 20$  minima corresponding to a spatial period  $\lambda = 2.3a_0$ . The competition between the driving force and landscape potential can produce a variety of hopping patterns in the particle motion. The relative values of  $F^{ac}$ ,  $F^{dc}$  and  $A_p$  control the rate and distance a particle moves forward and backward in the landscape. When  $F^d(t) > A_p$ , a particle can overcome the barrier height of the landscape, and the particle hops between

TABLE I: Simulation parameters and units with comparable experimental values [27, 28].

Quantity	Simulation Unit	Experimental value
length	$a_0 = 1$	$a_0 \sim 1.5\mu\text{m}$
energy	$E_0 = 1$	
force	$F_0 = E_0/a_0$	
time	$\tau = \eta a_0/F_0$	$\tau \sim 3\text{sec}$
velocity	$a_0/\tau$	$v \sim 5\mu\text{m/s}$
substrate period	$\lambda = 2.3a_0$	$\lambda = 3.5\mu\text{m}$
substrate amplitude <sup>a</sup>	$A_p = 0.1F_0$	$U_0 = 25k_B T \sim 1J$
temperature <sup>b</sup>	$T_0 = 0$	$T \sim 290K$

<sup>a</sup>Our substrate is scaled by our force units, while an experimental landscape is scaled by the Brownian motion of particles.

<sup>b</sup>To learn more about the effects of temperature on this simulation see Ex. IV D where we study  $U_0 \sim k_B T$ .

minima in the energy landscape. When the driving frequency is low, as in Fig. 2, the driven particle moves in a pattern with the same frequency as the time-dependent force  $F^d(t)$ , yet is modulated by the landscape period. We explore changes in frequency and  $F^{ac}$  in Ex. IV E. Here we vary  $F^{dc}$  while holding the remaining parameters fixed.

In Fig. 2(a) we plot  $F^d(t)$  as a function of time with constants  $F^{dc} = 0.07$ ,  $F^{ac} = 0.07$  and  $f = 0.01$  cycles per time unit  $\tau$ . The temporal period of the driving force is  $T = 1/f = 100\tau$  and the simulation has a maximum time of  $400\tau$ . In Fig. 2(b) we show the  $y$ -position of the particle as a function of time, where we normalize  $y$  by  $\lambda$ . The initial particle position is  $y = 0$ . The particle moves in the positive  $y$ -direction through  $\Delta y = \lambda$  over time  $T$ , with the average velocity  $\langle v_y \rangle = \lambda f$ . The inset of Fig. 2(b) shows  $y$  over one period  $100\tau < t < 200\tau$  with the contour plot described in Fig. 1(a). The motion is synchronized so the driving force is maximum when the landscape force is minimum, as shown by the coincidence of the steep slope in  $y/\lambda$  and maxima in  $F^d(t)$ . When  $F^d(t)$  is large the particle moves across the substrate minima, shown in blue with the contour plot. The slope of  $y/\lambda$  is zero twice during a driving period, indicating zero forward motion due to a coincidence of negative driving force and motion over the landscape maxima.

To explore the possible hopping patterns, we sweep through a range of  $F^{dc}$  for fixed  $F^{ac}$  and  $A_p$ . In Fig. 3 we increase  $F^{dc}$  in increments of  $0.001F_0$  and measure the average velocity  $\langle v_y \rangle$  as a function of  $F^{dc}$ . We perform the sweep for a non-oscillatory drive  $F^{ac} = 0.0$ . With no oscillating component of the driving force, the force-velocity relationship is monotonically increasing above the depinning threshold  $F^c$  such that

$$\langle v_y \rangle \propto (F^{dc} - F^c)^{-\beta}. \quad (6)$$

The critical force  $F^c$  is equal to the maximum substrate force  $A_p$  so the applied driving force can move a particle over a substrate barrier. The addition of an  $ac$  drive

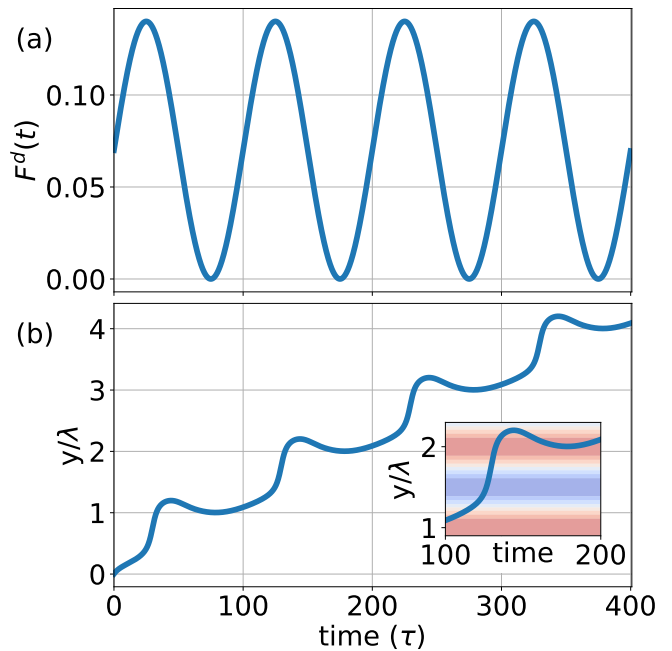


FIG. 2: (a) The applied driving force  $F^d(t)$  with parameters  $F^{dc} = 0.07$ ,  $F^{ac} = 0.07$  and  $f = 0.01$ . (b) The  $y$ -position of the driven particle normalized by the period of the substrate  $\lambda$ . The substrate strength is  $A_p = 0.1$ . The inset of (b) shows the  $y$ -position through the second period  $100\tau < t < 200\tau$  against the contour plot depicting the landscape potential described in Fig. 1(a).

leads to the formation of modes. A mode is a periodic pattern of hops with a constant average particle velocity,  $\langle v_y \rangle$  over a range of driving forces  $F^{dc}$ . In Fig. 3 we sweep  $F^{dc}$  with  $F^{ac} = 0.07$  and  $f = 0.01$ . Each step represents a different pattern of hops between substrate minima performed by the particle due to the landscape confinement. At low  $F^{dc}$  the average velocity  $\langle v_y \rangle$  is zero. Since  $A_p$  is large compared to the extrema of  $F^d(t)$ , the particle oscillates back and forth in a single minima with no net velocity. At higher  $F^{dc}$  the particle velocity  $\langle v_y \rangle$  increases in steps of uniform height,  $\langle v_y \rangle = n\lambda f$ , where  $n$  is an integer. The step width is non-linear and depends on the strength of  $F^{ac}$  as a Bessel function for this landscape potential [22, 28]. Known at Shapiro steps, these can have a variety of interesting patterns such as a devil's staircase related to chaotic dynamics [12].

To study synchronization patterns, it is useful to compare mode-locked quantities in a two dimensional phase plot. In a non-driven system, an appropriate phase space is particle velocity  $v_y$  versus position  $y$ . For a particle driven parallel to the  $y$ -direction, we define phase variables to account for the net increase in velocity and position. The phase position is defined as

$$\phi(t) = 2\pi(y(t) - \langle v_y \rangle t)/\lambda \quad (7)$$

centered about the average particle displacement  $\langle v_y \rangle t$  and normalized by the substrate period  $\lambda$  [27]. For clarity

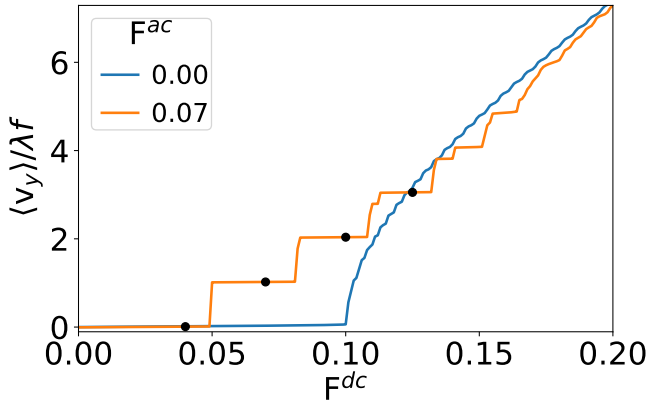


FIG. 3: Average particle velocity  $\langle v_y \rangle$  as a function of  $F^{dc}$ , the constant parameter of  $F^d(t)$  defined in Eq. 2. We fix  $F^{ac} = 0.0$  (blue) and  $F^{ac} = 0.07$  (orange) with  $f = 0.01$  as in Fig. 2. Each of the first four steps has a marked value of  $F^{dc}$ , indicating a system plotted in Fig. 4.

our plots are normalized by the prefactor  $2\pi$ . The phase velocity is

$$\dot{\phi}(t) = 2\pi(v_y(t) - \langle v_y \rangle) / \lambda. \quad (8)$$

With no landscape force, the phase velocity will be zero when  $F^d(t) = F^{dc}$ . When velocity is mode-locked to a spatial location a closed loop appears in phase space. The pattern is determined by the mode, or frequency ratio, so a 1:1 mode appears as a circle or oval. Nodes appear for higher modes, sometimes forming figure-eights or other recognizable patterns. A system that is nearly phase locked will appear as an unclosed loop. Such quasiperiodic systems are not fully synchronized so the position-velocity relationship shifts in time. In Fig. 4, all cases exhibit some line thickening, indicating the particle location and velocity are not fully synchronized, although this can be tuned by calculating  $\langle v_y \rangle$  over shorter time ranges.

In Fig. 4 we plot  $\dot{\phi}(t)$  versus  $\phi(t)$  for increasing  $F^{dc}$ , with the remaining parameters fixed as in Fig. 2. In Fig. 4(a) with  $F^{dc} = 0.04$  the phase plot is a small closed oval centered at  $(\phi, \dot{\phi}) = (0.1, 0)$ . A small tail appears due to the initial transient motion of the particle. The particle is confined in a single substrate minima, and has no net velocity. In Fig. 4(b) with  $F^{dc} = 0.07$  the phase loop is a symmetric triangular shape, indicating a 1:1 match between particle motion and velocity consistent with Fig. 2(a). The maximum  $\dot{\phi}$  occurs at  $\phi \sim 0.4$ , and maximum  $\phi$  occurs when  $\dot{\phi} \sim 0$ .

As  $F^{dc}$  increases, nodes form in the phase diagram that occur due to repeated values of  $\dot{\phi}$  over multiple phase positions. The motion becomes quasiperiodic so the loops in phase space do not fully overlap. In Fig. 4(c) with  $F^{dc} = 0.1$  two nodes form. The particle moves across  $2\lambda$  during one time period. In Fig. 4(d) with  $F^{dc} = 0.125$  three nodes form as the particle moves across  $3\lambda$ .

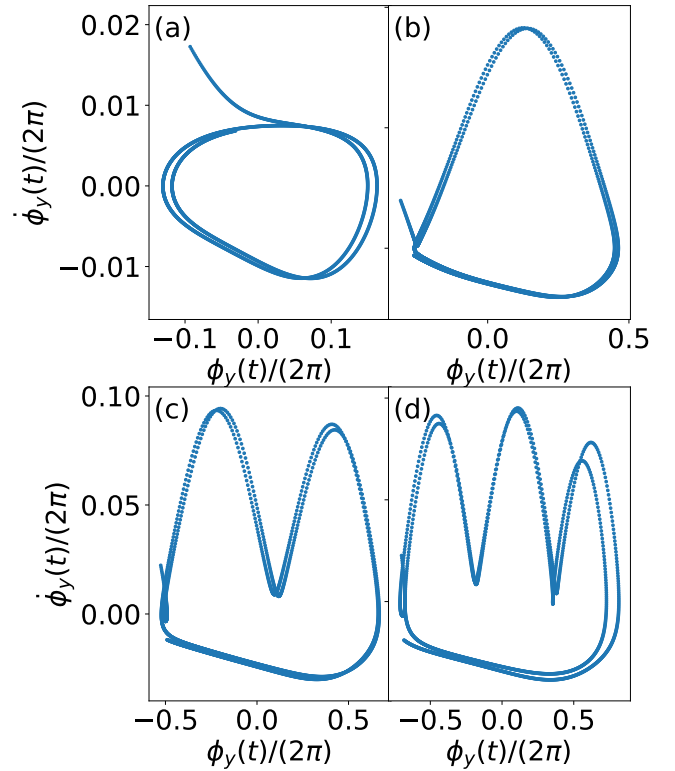


FIG. 4: Phase plot of a particle with  $F^{dc} =$  (a) 0.04, (b) 0.07, (c) 0.1, (d) 0.125. These values are marked as black circles in Fig. 3. The other parameters are  $F^{ac} = 0.07$ ,  $f = 0.01$ , and  $A_p = 0.1$  as Fig. 2.

In Section IV we explore our model with suggested exercises for interested readers. We include analytic exercises to examine the to linear drag equation in Ex. IV A, the equation of motion in Ex. IV B, and numerical integration techniques in Ex. IV C. We extend the model with numerical exercises to include finite temperature effects in Ex. IV D. We explore changes in the particle motion with parameter changes in Ex. IV E.

## IV. ASSOCIATED PROBLEMS

### A. Drag Models and Reynolds Numbers.

Stokes' law describes the drag force  $\vec{F}^{lin} = -3\pi\eta D\vec{v}$  on a sphere moving through a viscous liquid at velocity  $\vec{v}$  where  $\eta$  is the dynamic fluid viscosity and  $D$  is the particle diameter [39]. In simulation we subsume the constants  $3\pi D$  such that  $3\pi D\eta \rightarrow \eta$ . Often drag forces are modeled as a polynomial series [39]

$$\vec{F}^{drag} = -b\vec{v} - cv^2\hat{v} + \dots \quad (9)$$

Truncating the series to the first term is justified by demonstrating the sphere has a low Reynolds number  $R = Dv\rho/\eta$  where  $\rho$  is the fluid density and  $v$  the particle's speed. When  $R$  is small, the quadratic and higher

order terms may be ignored in favor of the linear drag term.

To first order the viscosity is  $\eta \sim 10^{-3}$  Pa-s [33]. **Using reasonable values for the experimental analog of this system, show that the Reynolds number is small.** In addition to the values listed in Table I, the liquid density  $\rho \sim 10^3$  kg/cm<sup>3</sup> is a reasonable first order approximation [42].

### B. Equation of Motion

Newton's second law states that the acceleration of a particle  $i$  is proportional to the sum of forces on the particle

$$m_i \vec{a}_i = \sum \vec{F}_i \quad (10)$$

where the constant of proportionality is the inertial mass  $m_i$ . The addition of a dissipative force to a dynamical equation of colloid motion is typically modeled with a drag force proportional to the particle's velocity in the opposite direction of motion  $\vec{F}^{drag} = -\gamma \vec{v}_i$  where  $\gamma = 3\pi\eta D$  is the drag coefficient described in Ex. IV A. The ratio of  $m/\gamma$  is known as the momentum relaxation time, and is small for particles with low Reynolds numbers. The mass of a typical colloid particle is 15 picograms, leading to a momentum relaxation time on the order of microseconds. **Confirm for the values listed in Table I, the momentum relaxation time is  $m/\gamma \approx 0.5 \mu s$ .**

When  $m/\gamma$  is small, particle acceleration can be ignored entirely. (a) Using Newton's Second Law for a small momentum relaxation time, **show that a particle confined to a landscape exerting force  $F^l(\vec{r}_i)$  subject to a time dependent drive  $F^d(t)$  can be modeled with the equation of motion described in Eq. 3.**

### C. Integration Methods

To calculate the position of the particle we integrate the equation of motion using the standard definition of velocity  $\vec{v}_i = d\vec{r}_i/dt$  via the Euler method. Our equation of motion provides a direct calculation for particle velocity, as demonstrated in Ex. IV B. When solving ordinary differential equations, the Euler method is effective for solving linear equations of the form  $dy/dt = f(t, y(t))$  with initial condition  $y(t_0) = y_0$ . The solution is calculated algorithmically by stepping in time through  $n$  integer steps  $t_n = t_0 + n\Delta t$ . At each subsequent step the new value for  $y$  is calculated as a map solution using discrete times  $y_{n+1} = y_n + f(t_n, y_n)$ . **Apply the Euler method to our equation of motion to solve for the analytic expression of position of a particle  $y_n$  at the  $n$ th timestep (i.e. Eq. 4).**

The Euler method can be applied to calculate reasonable numerical solutions to non-linear equations if

the time step  $\Delta t$  is kept sufficiently small [40]. In our simulations we use the timestep  $\Delta t = 0.1$  and find no change in the solution when we decrease the timestep to smaller values. In simulations including many interacting particles, a small timestep is essential for accurate models. Particle-particle interactions are typically non-linear, so the interparticle force changes significantly over small distances. Often molecular dynamics algorithms are solved with higher order methods such as the Verlet or Runge-Kutta methods. These methods include higher order terms that provide accurate solutions for second order differential equations, i.e.  $dy/dt = v$  and  $dv/dt = f_2(y, t)$ . In Newton's second law  $f_2$  would be proportional to the net force on a single particle. In our model we do not integrate  $f_2(y, t)$  since  $a = dv/dt = 0$ , as described in Ex. IV B.

### D. Brownian motion

Brownian motion is a phenomena in which visible particles change direction, apparently at random, due to collisions with invisible fluid particles. The rate of collisions depends on the temperature, viscosity and density of the suspending fluid. At higher temperatures the increased kinetic energy of particles makes collisions more likely, as described by the Maxwell-Boltzmann distribution [43]. An optically trapped colloid executing Brownian motion is a useful probe of microscopic forces [33].

In molecular dynamics simulations it is common to treat the invisible fluid particles as a continuous substance to reduce computational expense. Temperature effects can be modeled by applying randomized forces  $f^T$  to the visible particles. We use the normal distribution from the NumPy random module to generate a series of  $f_n^T$  values for each integer timestep  $n$  [44]. A normalized random distribution of forces causes fluctuations in motion equally in all directions such that the force  $f^T$  averaged over a finite time interval is zero. In one dimension this is expressed as

$$\langle f^T(t) \rangle = \frac{1}{N} \sum_n^N f_n^T = 0 \quad (11)$$

where  $n$  is an integer indicating discrete simulation timesteps and  $t = N\Delta t$ . A particle with sufficient energy  $k_b T_{min}$  may hop over landscape barriers. In our simulations, we define temperature as  $k_b T/E_0 \rightarrow T$  with constants set to unity to compare directly with force.

**With no applied driving force, find the minimum temperature required for a single particle to hop over maxima in the potential landscape.** Assume the particle is confined to move along the  $y$ -direction, include Brownian motion in the model.

In Fig. 5 we show the position versus time of a particle confined to a sinusoidal landscape undergoing Brownian motion. We increase the temperature relative to

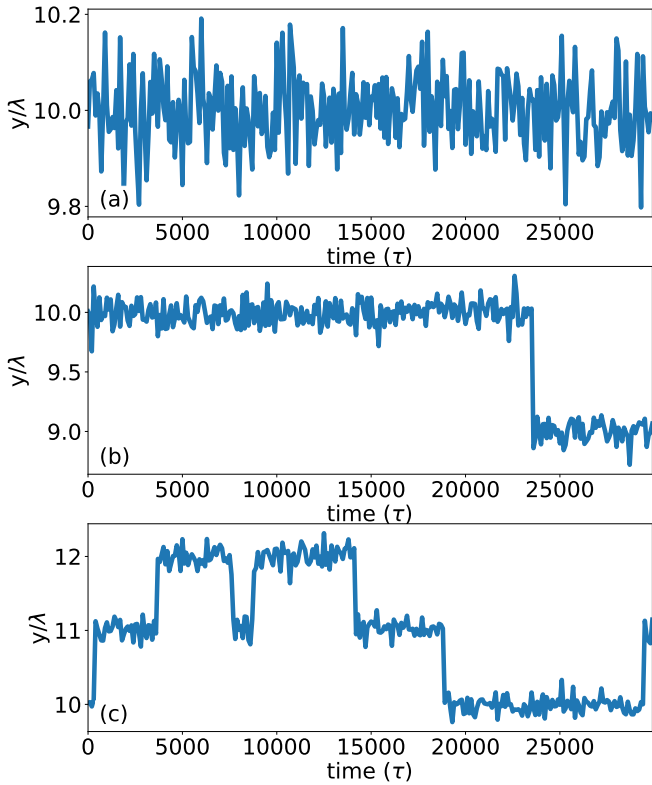


FIG. 5: Motion of a particle undergoing Brownian motion on a washboard potential energy landscape. (a)  $T/A_p = 3.0$  no hopping occurs. (b)  $T/A_p = 3.5$  one hop occurs and (c)  $T/A_p = 4.0$  many hops occur. Note the scale of the  $y$ -axis differs in each panel and the time scale is greater than in Fig. 2. The precise timing of hops pattern varies by simulation, sometimes exhibiting several hops for  $T/A_p = 3.5$ .

the amplitude of the landscape troughs until the particle enters a hopping regime. In Fig. 5(a) the temperature is  $T/A_p = 4.0$ . The particle executes a random walk centered at the potential minima  $y/\lambda = 10$ . We ran many simulations and never observed a hop to another minima within this simulation time. In Fig. 5(b)  $T/A_p = 5.0$ , hops between potential minima are possible but not probable, a back-forth hop occurs from  $y/\lambda = 10$  to 12 at  $t \sim 40000\tau$  and a single hop from  $y/\lambda = 10$  to 8 occurs at  $t \sim 280000\tau$ . In other simulations with identical parameters, we sometimes observed no hops or two hops between minima, as expected with random fluctuating systems. In Fig. 5(c)  $T/A_p = 6.0$  we observe many hops. The random thermalized kicks are sufficiently large to make the particle perform what appears to be a random walk of hops atop the substrate. [prove it]

For a driven particle, we ignore the effects of temperature in these simulations. We note that even at  $T/A_p = 6.0$  the hopping rate is much less than the frequency of the applied drive. This can be seen in the time scale in Fig. 5, where the average hopping rate is approximately every  $15000\tau$ , a value much larger than  $T = 100\tau$ . At sufficiently high temperatures, Brownian

motion does affect the formation of mode-locked steps and can be observed in experiments.

### E. Exploring Parameters of the Model

A range of oscillation behaviors can be explored by varying the relative strength of the confining landscape and external driving force. For the single driven particle, the hopping patterns are typically characterized by  $n_f$  the number of steps forward versus  $n_b$  the number of steps backward within a single time period. The total displacement of  $(n_f - n_b)\lambda$  is the net hop length. In Fig. 2, the particle moves forward through two minima ( $n_f = 2$ ), and does not move backward a full minima ( $n_b = 0$ ). In order to achieve backwards hops, the driving parameters must have a ratio of  $F^{ac}/F^{dc} > 1$  and a difference  $|F^{ac} - F^{dc}| > A_p$ . The frequency must be sufficiently low so that the applied force is large over a sustained time interval, allowing a particle to hop a substrate maxima. **Explore the effect changing the driving frequency on the hopping pattern.**

Fig. 6 shows the effects of lowering the frequency of applied driving force. We hold the remaining parameters fixed to  $F^{dc} = 0.1$ ,  $F^{ac} = 0.05$ , and  $A_p = 0.1$ . We observe no backward steps ( $n_b = 0$ ) across a broad range of frequencies since  $F^{dc} - F^{ac} = 0.05$  is too small to overcome  $A_p$ . The rate of forward hops increases as frequency decreases, but in each case the particle hops across two substrate periods as in Fig. 2. In Fig. 6(a-b) the particle hopping rate do not match the temporal period of  $F^d(t)$  due to the high frequency. In Fig. 6(a) the high frequency  $f = 0.1$  is apparent in the undulations of the particle with a period of  $10\tau$ . The particle is trapped between substrate minima  $y \approx \lambda/2$  for a time interval of  $400\tau$ . In Fig. 6(b) the frequency  $f = 0.05$  with a period of  $20\tau$  arrests the particle between minima, with a hopping rate of  $200\tau$ . At intermediate frequencies such as  $f = 0.01$  the particles are synchronized so that the hopping rate matches the driving frequency. In Fig. 6(c)  $f = 0.015$  the particle hops forward two minima every  $67\tau$ . Low frequencies result in sustained positive motion of a particle. In Fig. 6(d)  $f = 0.005$  the particle executes two subsequent forward hops before becoming trapped for the remainder of the period  $200\tau$ . In Fig. 6(e)  $f = 0.001$  the hopping is continuous over the simulation time. Here the particle reaches the top edge of the system and wraps back to  $y = 0$ . Given a simulation time of the period length  $1000\tau$ , the particle would cease forward motion.

Hopping patterns with backward steps are more difficult to achieve than forward. In Ref.[27] experiments with single colloids produce the following combinations of forward and backwards steps:  $n_f = 0$  to 6 for  $n_b = 0$ ,  $n_f = 0$  to 5 for  $n_b = -1$ , and  $n_f = 2$  to 3 for  $n_b = -2$  by sweeping through a variety of applied forces parameters  $F^{dc}$  and  $F^{ac}$ . **Find the parameters that create hopping patterns similar to those in Ref. [27].**



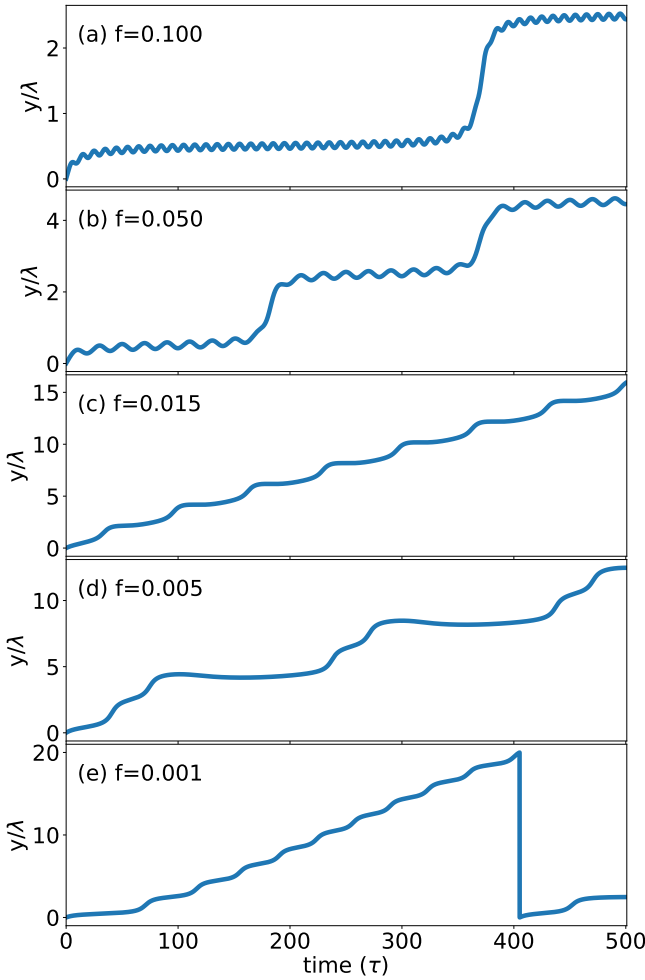


FIG. 6: Motion of a particle with the same values of  $F^{dc} = 0.1$  and  $F^{ac} = 0.05$  as Fig. 2 and decreasing frequency  $f =$  (a) 0.1, (b) 0.05, (c) 0.015, (d) 0.005 and (e) 0.001 where the particle wraps the periodic boundary conditions.

In Fig. 7 we explore a hopping pattern not observed in Ref. [27]. This is possible in simulation because our particle readily hops through  $2\lambda$ . We fix  $f = 0.01$ ,  $F^{dc} = 0.1$ , and  $A_p = 0.1$  and increase the amplitude of  $F^{ac}$ , which causes the number of backwards steps to increase. The number of forward steps also increases due to the increased total positive amplitude of  $F^d(t)$ . In Fig. 7(a)  $F^{ac} = 0.2$ , the number of backwards steps  $n_b = 0$  with  $n_f = 6$ . In Fig. 7(b)  $n_b = 2$  and  $n_f = 8$ . In Fig. 7(c)  $n_b = 4$  and  $n_f = 10$ . In each case the average velocity is  $\langle v_y \rangle = 6\lambda/T$ .

In Fig. 8 we sweep the constant driving force  $F^{dc}$  for a fixed amplitude  $F^{ac}$  and frequency  $f = 0.01$ . In the high frequency limit, the steps are separated by linearly increasing regions.

Fig. 8(a) shows  $F^{ac} = 0.0$  and (b) shows  $F^{ac} = 0.4$  with frequency  $f = 0.01$ .

The particle does not phase lock since there is no periodicity to  $F^d(t)$ , but does exhibit undulations in  $\langle v_y \rangle$  due

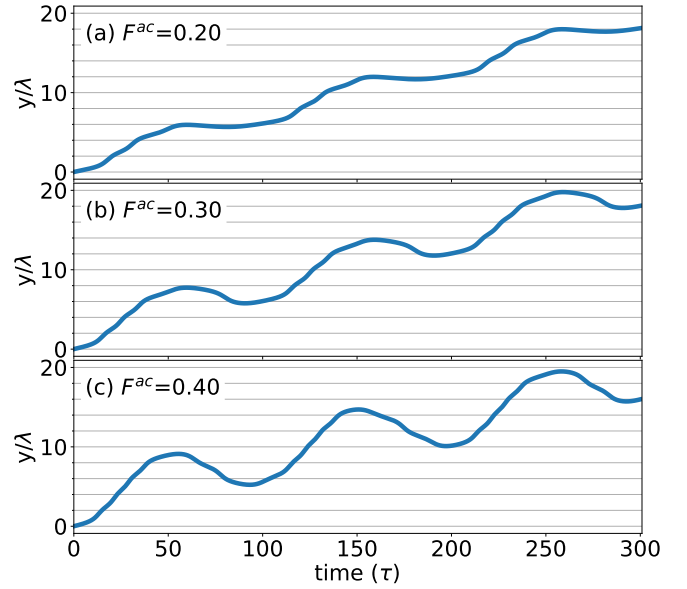


FIG. 7: Motion of a particle with the same values of  $F^{dc}$  and frequency as Fig. 2 and increasing  $F^{ac}$ . (a) The particle moves forward six minima with no steps backward. (b) The particle moves forward eight minima with two steps backward. (c) The particle moves forward nine minima with four steps backward.

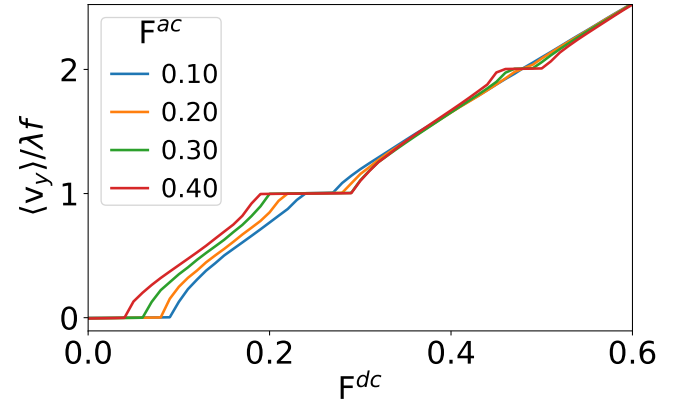


FIG. 8:  $\langle v_y \rangle$  vs.  $F^{dc}$  of a particle with  $F^{ac} = 0.1$  (blue),  $F^{ac} = 0.2$  (orange),  $F^{ac} = 0.1$  (green) and  $F^{ac} = 0.2$  (red) with frequency  $f = 0.0$ . The substrate is as in Fig. 2 with  $A_p = 0.1$ .

to the corrugations in the substrate. When  $F^{ac} = 0.4$ , mode-locked steps appear in  $\langle v_y \rangle$  vs.  $F^{dc}$ . At low values of  $F^{dc}$  the particle may move backwards, distorting the steps, as seen below  $F^{dc} < 0.3$ . Between  $0.3 < F^{dc} < 0.5$  the system exhibits phase locked steps.

## V. CONCLUSION

A single particle driven across a periodic potential landscape synchronizes its motion to environmental and

external forces, a phenomena known as mode-locking. Our simulations reproduce experiments and simulations presented in Juniper *et al.* [27, 28] of mode locking in driven colloids on a periodic optical landscape. Colloids are relatively easy to manipulate and image in experiments, making ideal proxies for systems such as cold atoms or electron gases [31]. Dynamical mode-locking is observed important technologies such as in quantum electronic devices as stepped regions in current-voltage (I-V) relationship, where voltage is the analog of external driving force and current is that of particle velocity. Known as Shapiro steps, these mode-locked or phase-locked currents have been observed due to applied ac voltages in single Josephson junctions [20, 23] and coupled arrays of junctions [21]. Shapiro steps vary in width depending on the strength of the applied ac forces, and are observed in a variety of ac and dc driven systems displaying non-Ohmic behavior in voltage-current curves, including charge waves, spin density waves and superconducting vortices in landscapes engineered with periodic patterns of pinning sites [22]. Mode-locking is a use-

ful probe of complex quantum mechanical systems since the motions of individual particles can only be inferred from other measurements. Our results can be relevant to synchronization effects in a broad range of experiments systems including optically confined colloids, superconductors with periodic pinning arrays, and the charge and spin of atomic systems.

## Acknowledgments

We acknowledge Harvey Gould and Jan Tobochnik, who invited us to write the article and supported its development. Charles and Cynthia Reichhardt advised the project and provided the original molecular dynamics code written in the C programming language. We acknowledge funding from the M.J. Murdock Charitable Trust and the Pacific Research Institute for Science and Mathematics.

- 
- [1] A. Pikovsky, M. Rosenblum, and J. Kurths, *Synchronization: A Universal Concept in Nonlinear Sciences* (Cambridge Univ. Press, Cambridge, 2003).
  - [2] M. Bennett, M.F. Schatz, H. Rockwood, and K. Wiesenfeld, Huygens' clocks, *Proc. Roy. Soc. A* **458**, 563 (2002).
  - [3] K. Okamoto, A. Kijima, Y. Umeno, and H. Shima. Synchronization in flickering of three-coupled candle flames. *Sci Rep* **6**, 36145 (2016)
  - [4] T. Arane, A. K. R. Musalem and M. Fridman, Coupling between two singing wineglasses, *Am. J. Phys.* **77**, 1066 (2009).
  - [5] J. Jia, Z. Song, W. Liu, J. Kurths, and Xiao, J. Experimental study of the triplet synchronization of coupled nonidentical mechanical metronomes. *Sci. Rep.* **5**, 17008 (2015).
  - [6] S. Portugal, T. Hubel, J. Fritz, S. Heese, D. Trobe, B. Voelkl, S. Hailes, A. M. Wilson and J. R. Usherwood. Upwash exploitation and downwash avoidance by flap phasing in ibis formation flight. *Nature* **505**, 399 (2014).
  - [7] I. Aihara, T. Mizumoto, T. Otsuka, H. Awano, K. Nagira, H. G. Okuno and K. Aihara. Spatio-Temporal Dynamics in Collective Frog Choruses Examined by Mathematical Modeling and Field Observations. *Sci Rep* **4**, 3891 (2014).
  - [8] P. Tranchant, D. T. Vuvan, and I. Peretz, Keeping the Beat: A Large Sample Study of Bouncing and Clapping to Music. *PLoS ONE* **11**(7): e0160178. (2016).
  - [9] G. Martin Hall, Sonya Bahar, and Daniel J. Gauthier, Prevalence of Rate-Dependent Behaviors in Cardiac Muscle. *Phys. Rev. Lett.* **82**, 2995 (1999).
  - [10] W. Singer. Striving for coherence. *Nature*, **397** 391, 1999.
  - [11] Dutta, S., Parihar, A., Khanna, A. et al. Programmable coupled oscillators for synchronized locomotion. *Nat Commun* **10**, 3299 (2019).
  - [12] P. Bak. The Devil's Staircase. *Physics Today* **39**, 12, 38 (1986).
  - [13] J. A. Lissajous. "Mmoire sur l'Etude optique des mouvements vibratoires," *Annales de chimie et de physique*, 3rd series, 51 (1857) 147-232
  - [14] E. Y. C. Tong, Lissajous figures, *The Physics Teacher* **35**, 491 (1997).
  - [15] A. Pertsinidis, and X. Ling, Equilibrium Configurations and Energetics of Point Defects in Two-Dimensional Colloidal Crystals. *Phys Rev Lett*, **87**, 098303 (2001).
  - [16] E. M. Purcell, Life at low Reynolds numbers, *Am. J. Phys.* **45**, 311 (1977).
  - [17] B. D. Josephson, *Phys. Letters* **16**, 25 (1962).
  - [18] B. D. Josephson, *Advan. Phys.* **14**, 419 (1965).
  - [19] W. C. Stewart, Current-Voltage Characteristics of Josephson Junctions, *Appl. Phys. Lett.* **12**, 277 (1968).
  - [20] S. Shapiro, Josephson currents in superconducting tunneling: the effect of microwaves and other observations, *Phys. Rev. Lett.* **11**, 80 (1963).
  - [21] S. P. Benz, M. S. Rzchowski, M. Tinkham, and C. J. Lobb, Fractional giant Shapiro steps and spatially correlated phase motion in 2D Josephson arrays, *Phys. Rev. Lett.* **64**, 693 (1990); D. Domínguez and J. V. José, Giant Shapiro steps with screening currents, *Phys. Rev. Lett.* **69**, 514 (1992).
  - [22] C. Reichhardt, R. T. Scalettar, G. T., Zimányi, N. Grønbech-Jensen, Phase-locking of vortex lattices interacting with periodic pinning. *Phys. Rev. B* **61**, R11914 (2000).
  - [23] A. A. Golubov, M. Yu. Kupriyanov, and E. Il'ichev. The current-phase relation in Josephson junctions, *Rev. Mod. Phys.* **76**, 411 (2004).
  - [24] Dengling Zhang, Haibo Qiu, and Antonio Muñoz Mateo, Unlocked-relative-phase states in arrays of Bose-Einstein condensates, *Phys. Rev. A* **101**, 063623 (2020).
  - [25] C. Reichhardt and C. J. Olson Reichhardt, Depinning and nonequilibrium dynamic phases of particle assemblies driven over random and ordered substrates: a review, *Rep. Prog. Phys.* **80**, 026501 (2017).



- [26] C. Reichhardt, and C. J. O. Reichhardt, Shapiro steps for skyrmion motion on a washboard potential with longitudinal and transverse ac drives. *Phys. Rev. B* **92**, (22). (2015).
- [27] M. P. N. Juniper, A. V. Straube, R. Besseling, D. G. A. L. Aarts, and R. P. A. Dullens, Microscopic dynamics of synchronization in driven colloids. *Nat. Commun.* **6**, 7187 (2015);
- [28] Juniper, M. P. N., Zimmermann, U., Straube, A. V., Besseling, R., Aarts, D. G. A. L., Löwen, H., and Dullens, R. P. A. Dynamic mode locking in a driven colloidal system: Experiments and theory. *New Journal of Physics*, 19(1). (2017).
- [29] S. Herrera-Velarde and R. Castañeda-Priego, Superparamagnetic colloids confined in narrow corrugated substrates, *Phys. Rev. E* **77**, 041407 (2008).
- [30] S. Herrera-Velarde and R. Castañeda-Priego, *J. Phys.: Condens. Matter* **19**, 226215 (2007).
- [31] D. G. Grier, A revolution in optical manipulation. *Nature* **424**, 810 (2003).
- [32] Arthur Ashkin, Optical trapping and manipulation of neutral particles using lasers, *Proc. Natl. Acad. Sci. U.S.A.* **94**, 48534860 (1997).
- [33] G. Volpe and G. Volpe, Simulation of a Brownian particle in an optical trap, *Am. J. Phys.* **81** (3), March 2013
- [34] C. Lutz, M. Kollmann, and C. Bechinger, *Phys. Rev. Lett.* **93**, 026001 (2004); C. Lutz, M. Kollmann, C. Bechinger, and P. Leiderer, *J. Phys.: Condens. Matter* **16**, S4075 (2004).
- [35] S. Tarucha, T. Honda, T. Saku, *Solid State Commun.* **1995**, 94, 413.
- [36] A. Gholami, O. Steinbock, V. Zykov, and E. Bodenschatz, Flow-Driven Waves and Phase-Locked Self-Organization in Quasi-One-Dimensional Colonies of *Dictyostelium discoideum*, *Phys. Rev. Lett.* **114**, 018103 (2015).
- [37] D. Frenkel and B. Smit, *Understanding Molecular Simulation: From Algorithms to Applications* (Academic Press, London, 2001).
- [38] M. P. Allen and D. J. Tildesley, *Computer Simulation of Liquids*. Second Edition. Oxford University Press (2017).
- [39] J. Taylor, *Classical mechanics*. University Science Books (2005).
- [40] M. Newman, *Computational Physics*, CreateSpace Independent Publishing Platform. (2012).
- [41] Supplementary videos coming soon.
- [42] IAPWS R12-08, Release on the IAPWS Formulation 2008 for the Viscosity of Ordinary Water Substance, September 2008, <http://www.iapws.org/relguide/viscosity.html>
- [43] A Einstein, *Investigations on the Theory of the Brownian Movement*, Dover Publications (1956).
- [44] C.R. Harris, K.J. Millman, S.J. van der Walt, et al. Array programming with NumPy. *Nature* **585**, 357 (2020).